Nuclear Inst. and Methods in Physics Research B xxx (xxxx) xxx–xxx

Contents lists available at ScienceDirect

Nuclear Inst. and Methods in Physics Research B

journal homepage: www.elsevier.com/locate/nimb

Status of the new fragment separator ACCULINNA-2 and first experiments

G. Kaminski[a,b,*], B. Zalewski[a,b], S.G. Belogurov[a], A.A. Bezbakh[a,c], D. Biare[a], V. Chudoba[a,d], A.S. Fomichev[a,e], E.M. Gazeeva[a], M.S. Golovkov[a,e], A.V. Gorshkov[a,c], L.V. Grigorenko[a,f,g], D.A. Kostyleva[a], S.A. Krupko[a,c], I.A. Muzalevsky[a,d], E.Yu. Nikolskii[a,f], Yu.L. Parfenova[a], P. Plucinski[a,h], A.M. Quynh[a,i], A. Serikov[a], S.I. Sidorchuk[a], R.S. Slepnev[a], P.G. Sharov[a,c], P. Szymkiewicz[a,h], A. Swiercz[a,h], S.V. Stepantsov[a], G.M. Ter-Akopian[a,e], R. Wolski[a,j]

[a] Joint Institute for Nuclear Research, 141980 Dubna, Russia
[b] Heavy Ion Laboratory, University of Warsaw, 02-093 Warsaw, Poland
[c] SSC RF ITEP of NRC "Kurchatov Institute", 117218 Moscow, Russia
[d] Institute of Physics, Silesian University in Opava, 746 01 Opava, Czech Republic
[e] Dubna State University, 141982 Dubna, Russia
[f] National Research Center "Kurchatov Institute", 123182 Moscow, Russia
[g] National Research Nuclear University "MEPhI", 115409 Moscow, Russia
[h] AGH University of Science and Technology, Faculty of Physics and Applied Computer Science, 30-059 Krakow, Poland
[i] Nuclear Research Institute, 670000 Dalat, Vietnam
[j] Institute of Nuclear Physics PAN, 31342 Krakow, Poland

ARTICLE INFO

Keywords:
Radioactive ion beams
In-flight separator
Energy degrader

ABSTRACT

The start of operation of a new separator ACCULINNA-2 makes an important upgrade for the Radioactive-Ion Beam (RIB) research done at the Flerov Laboratory of Nuclear Reactions (FLNR, JINR). Test results indicate that the separator meets the project specifications. Intensities obtained for the ^{6,8}He, ^{9,11}Li, ^{12}Be RIBs are 15 times higher in comparison with the results achieved at the old separator ACCULINNA. An overview of the design, construction and commissioning studies of the ACCULINNA-2 separator is presented. The separator will be equipped with some key facilities: a cryogenic tritium target, zero degree spectrometer following the physical target bombarded by the RIBs, and with a neutron detector array, and the Time Projection Chamber (TPC). This opens a wide range of experimental possibilities. Overview is presented on the two first experiments devoted to the study of d + ^{6}He elastic scattering and search for a ^{7}H low-lying resonance state populated in the ^{2}H (^{8}He,^{3}He)^{7}H reaction.

1. Introduction

ACCULINNA-2 is a part of the Dubna Radioactive Ion Beams (DRIBs) project [1–3]. It is a new in-flight facility installed at a primary beam line of the U-400M cyclotron for the study of exotic nuclear systems with atomic number $Z < 20$ [2,4]. The separator was commissioned in 2017 as a result of successful collaboration with the SIGMAPHI company [5]. The observed RIB characteristics (intensity, purity, beam profiles in all focal planes) are in agreement with the specification. The new separator provides high quality secondary beams and opens new opportunities for the experiments made with the RIBs of the intermediate energy range (10–50 *A*MeV) [3].

2. The ACCULINNA-2 separator

RIBs with atomic number $Z < 20$ at the ACCULINNA-2 separator are produced with the projectile fragmentation technique by impinging intermediate-energy primary beams (30–50 *A*MeV) on a production target (see, for example, early works [6,7] devoted to the fragmentation studies). The production target is usually a beryllium plate, 0.5–2-mm-thick, installed on a stationary or rotating target support cooled by water. By design, the ACCULINNA-2 is an achromatic ion optical system. The main parts of the separator are two 45° dipole magnets with a maximum magnetic rigidity of 3.9 Tm. The beam-line optics consists of 14 quadrupole and 8 multipole elements. The schematic layout of the separator at the cyclotron hall is presented in Fig. 1 (see also the drawn setup in [3]). The basic characteristics of the

* Corresponding author at: Joint Institute for Nuclear Research, 141980 Dubna, Russia.
E-mail address: kaminski@jinr.ru (G. Kaminski).

https://doi.org/10.1016/j.nimb.2019.03.042
Received 6 February 2019; Received in revised form 17 March 2019; Accepted 20 March 2019
0168-583X/

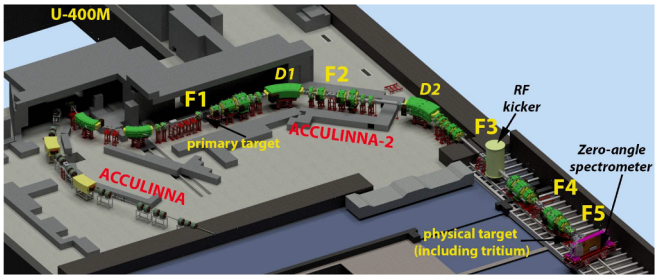

Fig. 1. Layout of the ACCULINNA and ACCULINNA-2 separators at the U-400M cyclotron hall.

Table 1
Basic characteristics of the ACCULINNA-2 separator, where $\Delta\Omega$ is the solid angle, δ_P – momentum acceptance, and $P/\Delta P$ – momentum resolution, respectively.

$\Delta\Omega$ (msr)	4.2
δ_P %	6.0
$P/\Delta P$	2000
$B\rho_{max}$ (Tm)	3.9
L (m)	37
E_{min} (AMeV)	5
E_{max} (AMeV)	50

ACCULINNA-2 separator are presented in Table 1.

Radioactive nuclei leaving the production target at the F1 focal plane are captured by a short-focusing quadrupole triplet Q1–Q3 and are transported through the magnetic dipoles D1–D2 and magnetic quadrupoles Q4–Q14 up to the final focal plane F5. Magnetic multipoles with corresponding sextupole and octupole components are used for correction of second- and third- order aberrations occurring otherwise in the F2 and F3 planes (see in Fig. 1). In Fig. 2 the beam envelopes calculated to the second order with the TRANSPORT code [8] are shown. In designing the ACCULINNA-2 ion optics, a major effort was made in searching for the optimum configuration achieving reasonable compromise between the separation efficiency, the beam acceptance and magnetic rigidity, considering the limits set by the existing infrastructure at the cyclotron hall, as well as technical limits and facility cost.

The purification of the reaction fragments is achieved by a

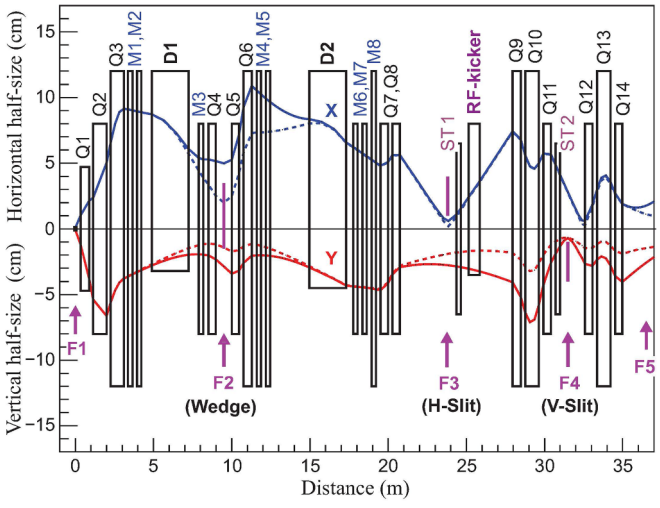

Fig. 2. Beam envelopes in horizontal (X) and vertical (Y) planes. The dimensions of the F1 object slit is 2×2 mm^2, capture angles are ±30 and ±35 mrad in X and Y planes, respectively. The solid lines are for $\delta_P = \pm2.5\%$ and dashed ones for $\delta_P = \pm1.0\%$ (taken from [3]).

separation method based on magnetic-rigidity analysis and energy-loss in a degrader material. The D1 dipole magnet filters fragments by their magnetic rigidity $B\rho$, providing dispersion at the focal plane F2. The relation between the magnetic rigidity of the first bending magnet and the A/Z number is given by $B\rho = p/q$. Further purification is achieved by separation of the fragments by their energy losses in the wedge-shaped degrader. The second dipole D2 compensates the dispersion occurring in the focal plane F2 and collects the fragments at the achromatic focal plane F3. Identification of the reaction products is performed by the measurement of the Time of Flight (TOF) and energy loss of the fragments. TOF is measured on the 12.3-meter flight path lying between the F3 and F5 focal planes. Silicone double-sided multi-strip detectors for energy loss (ΔE) measurement are installed in focal plane F5. The selection made for the thicknesses of the production target and wedge-shaped degrader in accord with the position determination made for the momentum slits standing in focal planes F2–F5 have direct influence on the yield and purity of the required RIB. This is typically sufficient for the production of quite pure RIBs of light, neutron-rich exotic nuclei. Proton-rich RIBs need additional purification from a large amount of contamination. The reason of that is the fragmentation mechanism leads to the low-energy tails of obtained in the energy spectra of the very well-produced undesirable less proton-rich nuclei. Adding the velocity separation to the magnetic-rigidity analysis one can drastically reduce the effect of this contamination. For this purpose a radio-frequency (RF) kicker will be installed in 2019 on the ACCULINNA-2 beam-line between the F3 and F4 focal planes (see in Fig. 1). Such RF-kickers operate well in different laboratories over the world [9–12].

3. First radioactive ion beams

The results of the commissioning of the ACCULINNA-2 fragment separator are reported in Ref. [3]. The primary beam of ^{15}N with energy of 49.7 AMeV was impinged on 2-mm-thick beryllium target. A 1-mm beryllium wedge shape degrader was installed at the dispersive focal plane F2. Individual radioactive nuclei were identified in the obtained RIB cocktail by the TOF and energy-loss measurement. The TOF detector consisted of a couple of plastic scintillators BC404, 250-μm-thick, and 60 mm in diameter in the sensitive area. The 0.3-mm-thick double-sided strip silicon detector (Micron-Semiconductor, type BB7) with sensitive area 64×64 mm^2, and with 32 strips on each side, was located behind the second TOF detector in the F5 plane and was used for the secondary-beam profile and energy-loss measurements (later on, in full-scale experiments, the plastic scintillators and multi-wire proportional chambers were used). Examples of typical two-dimensional identification plots, energy loss ΔE versus TOF, are presented in Ref. [3,13].

Main parameters measured for several light neutron-rich RIBs in the final focal plane F5 are presented in Table 2. These initial operation tests were done for a choice of neutron-rich RIBs prospective for the first-day experiments planned at the ACCULINNA-2 separator. The tests were performed with the primary-beams intensity limited at a level of no more than 100 particle nano-Amperes (pnA) due to absence of a proper radiation protection in the production-target area. Since 2018,

Table 2
Main parameters obtained for several light neutron-rich RIBs in final focus F5. Data were obtained using the 100-pnA primary beam of ^{15}N for the momentum acceptance of ±2%, 1-mm beryllium wedge put in dispersive plane F2, and ±11-mm slit in F3. The primary-beam intensity was limited by the lack of concrete shielding around the F1-F2 area.

RIB	^{14}B	^{12}Be	^{11}Li	^{9}Li	^{8}He
Energy, AMeV	37.7	39.4	37.0	33.1	35.8
Intensity, 1/s	1.2×10^4	1.5×10^4	4×10^2	1.1×10^5	2.5×10^3
Purity, %	65	92	67	51	89

Table 3
Main parameters of zero-angle dipole.

Maximum field	(T)	1.44
Minimum field	(T)	0.4
Effective length for B = 1.2 T	(mm)	524
Gap	(mm)	180
Good field region dimensions	(±mm)	250/75
Field homogeneity for B = 1.2 T		0.003

after installation of the concrete shield around the separator, RIBs are produced at maximum current of primary beam intensity, up to 4 pμA. The list of primary beams of the U-400M cyclotron available for the RIB experiments [14] can be found in Ref. [3].

4. ACCULINNA-2 instrumentation

In order to extend experimental opportunities ACCULINNA-2 is being equipped with new instruments: i) zero-angle spectrometer and particle-tracking system, ii) RF-kicker for the purification of proton-rich beams, iii) cryogenic target system [15], iv) neutron spectrometer [16], v) Optical Time Projection Chamber (OTPC) [17].

The zero-angle spectrometer was commissioned in 2017. It will considerably improve the cumulative energy resolution of the experiments with the observation of beam-like products or recoils in case of high RIB intensity. The principal parameters of this dipole magnet are listed in Table 3. It will provide precise detection of recoil fragments typically emitted at the decay of exotic nuclei situated near and beyond the drip lines. These so far little-studied nuclear systems make the main subject of study at ACCULINNA-2. The major destination of the spectrometer is to enhance the quality of spectroscopic data arriving from ACCULINNA-2 for the exotic nuclei, such as ^{7}H, ^{10}He, ^{16}Be, ^{17}Ne and ^{26}S [1–3,14]. At present a particle tracking detector array [16] is being developed for the zero-angle spectrometer.

In the area following after the achromatic focal plane F3, the vertically deflecting radio-frequency (RF) kicker will be installed. Its main parameters are presented in Table 4.

5. First experiments

During the last three decades the research associated with the use of RIBs led to the discovery of several new phenomena taking place in the region of weakly bound nuclei. The list of new findings involves the discovery of neutron halo and neutron skin structures, the specific many-body correlations, the low-lying resonant states observed in the nuclei lying close to the neutron drip-line. However, new experimental data in this field are needed very much. In particular, in spite of numerous experiments carried out with the exotic ^{6}He nucleus, the interaction between two weakly bound systems the ^{6}He and deuteron has not been studied so far. Meanwhile, the optical potentials involving ^{6}He and its low-energy spectrum attract strong attention (see e.g. [18,19]). For this purpose, as an initial experiment at ACCULINNA-2, the measurements of ^{6}He-*d* elastic and inelastic scattering were carried out. Angular distributions for elastic and inelastic scattering were obtained

Table 4
Main characteristics of RF-kicker.

Electrode vertical gap, 2*h* (cm)	7
Electrode width, 2*w* (cm)	12
Electrode length, *L* (cm)	70
Cylinder diameter, *D* (cm)	120
Length of coaxial line, *H* (cm)	183
Electric field amplitude (kV/cm)	15
Frequency range, *f* (MHz)	15–22

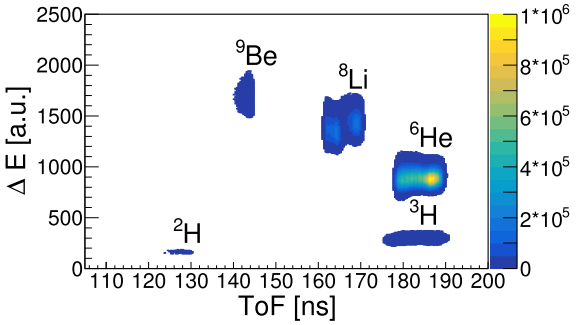

Fig. 3. Identification plot showing the energy loss in plastic scintillator (250 μm thick) versus TOF in the F5 plane at the setting made for the ^{6}He beam with energy 26 *A*MeV.

in the angular range of 25° – 130° in the center-of-mass (CM) system.

The ^{6}He beam was produced in fragmentation of ^{15}N with energy of 49.7 *A*MeV on 2 mm beryllium target. The separator provides 78% pure secondary ^{6}He beam at 26 *A*MeV with intensity of ~10^{5} pps. The beam energy was determined by TOF at 12.3 m base, while ion identification was performed with the use of standard Δ*E* – TOF technique. An example of Δ*E* – TOF identification plot obtained when tuning was made for the ^{6}He beam is presented in Fig. 3.

The beam tracking on the target was performed with Multi-Wire Proportional Chambers (MWPC) [20,21]. The beam spot on the target was 17 mm in diameter (FWHM). As a target, 100 μm foil made of deuterized polyethylene was used. The schematic drawing of the experimental setup and preliminary results are presented in Figs. 4 and 5, respectively.

The measurement of inelastic ^{6}He – d scattering was performed by the detection of deuterons in the coincidence with alpha-particles emitted during the decay of ^{6}He excited states. It may allow to observe not only the spectrum, but also to extract information about spin and parity of these states from the analysis of angular correlations. Coincidence of deuterons in the *d*-telescope with ^{6}He in the He-telescope was determined as the best way to identify the elastic-scattering process. The statistics obtained after normalization to the number of particles impinging on the physical target is presented in Fig. 5 as a function of CM angle. The decrease of detection efficiency on the edges for each of the three d-telescope settings, leads to the decrease of the statistics in these areas. The experimental setup used for the study allows for in-depth investigation of optical potential through the elastic scattering measurements and subsequently extracted differential cross sections.

Recently, the first run aimed at the study of superheavy ^{7}H produced in the transfer reaction ^{2}H(^{8}He,^{3}He)^{7}H with 26 *A*MeV ^{8}He beam bombarding deuterium gas cryogenic target (6 mm thick at 27 K and at 1 atm) was performed. The idea of the measurement was to obtain more

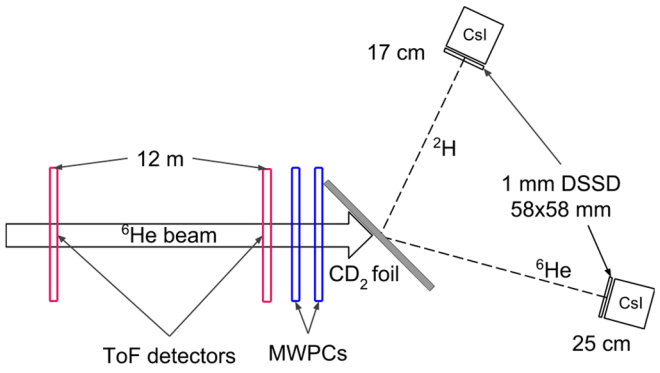

Fig. 4. Schematic view of the experimental setup for the measurements performed for the ^{6}He– *d* elastic and inelastic scattering.

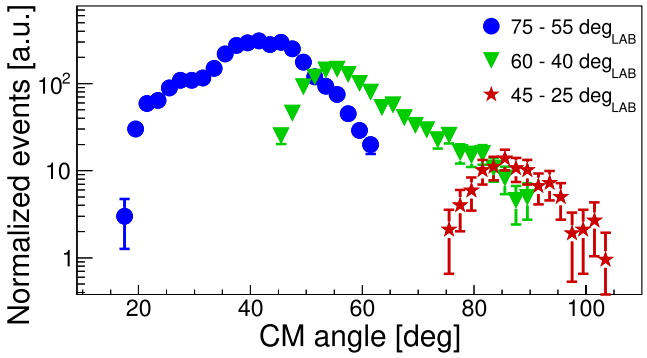

Fig. 5. Normalized event numbers obtained at different CM angles for the elastic scattering channel ^{2}H(^{6}He,^{6}He) at E_{CM} = 39 MeV. Different colors correspond to results obtained at three different angular settings of the d-telescope.

statistics and better missing mass energy resolution than in Ref [22], and to collect correlation data which one could obtain for the ^{7}H→t + 4n decay by measuring the energies and angles of tritons and neutrons. To detect the ^{3}He recoil nuclei two silicon telescopes consisting of 22 μm and 1-mm-thick silicon strip detectors were used. The energies and positions of tritons from the decay ^{7}H→t + 4n were measured at forward angles by $\Delta E - E$ telescope consisting of a double-sided 1.5-mm-thick silicon strip detector and CsI(Tl)/PMT array (4 by 4 modules). The data analysis is in progress.

6. Conclusions

The commissioning phase of the ACCULINNA-2 fragment separator at the FLNR, JINR U-400M cyclotron is accomplished. The first radioactive beams are obtained. The basic ion-optical characteristics of ACCULINNA-2 are confirmed experimentally for a number of RIBs. The first-day experiments devoted to the study of ^{6}He + d scattering and to the search for the ^{7}H nucleus were carried out. Several experiments implying the study of such exotic nuclei as ^{10}Li, ^{7}H, ^{17}Ne and ^{26}S are planned to be performed at this facility in the near future after the upgrade of the U-400M cyclotron scheduled to be done in 2019-2020.

Acknowledgment

This work was partly supported by Russian Science Foundation grant 17-12-01367.

References

[1] http://aculina.jinr.ru/acc-2.php.
[2] L.V. Grigorenko, et al., Physics – Uspekhi 59 (2016) 321.
[3] A.S. Fomichev, et al., Eur. Phys. J. A 54 (2018) 97.
[4] http://flerovlab.jinr.ru/flnr/u400m.html.
[5] https://www.sigmaphi.fr.
[6] D.E. Greiner, et al., Phys. Rev. Lett. 35 (1975) 152.
[7] H.H. Heckman, et al., Phys. Rev. C 17 (1978) 1735.
[8] K.L. Brown, et al., TRANSPORT, Report CERN 80-04, Geneva (1980).
[9] K.E.G. Lijbner, et al., Nucl. Instrum. Methods Phys. Res. B 301 (1987) 301.
[10] K. Yamadaa, T. Motobayashi, I. Tanihata, Nucl. Phys. A 746 (2004) 156c.
[11] D. Bazin, et al., Nucl. Instrum. Methods Phys. Res. A 606 (2009) 341.
[12] R.C. Pardo, et al., Nucl. Instrum. Methods Phys. Res. A 790 (2015) 1.
[13] A.A. Bezbakh, et al., EPJ Web Conf. 177 (2018) 03001.
[14] G.M. Ter-Akopian, Yu.E. Penionzhkevich, Yu.G. Sobolev (Eds.), Proc. Int. Symp. on Exotic Nuclei, EXON-2016, World Scientific, Singapore, 2017, pp. 380–389 ISBN 978-981-3226-53-1.
[15] A.A. Yukhimchuk, et al., Nucl. Instrum. Methods Phys. Res. A 513 (2003) 439.
[16] A.A. Bezbakh, et al., Instrum. Exp. Tech. 61 (2018) 631.
[17] M. Pomorski, et al., Phys. Rev. C 90 (2014) 014311 .
[18] L. Yang, et al., Phys. Rev. Lett. 119 (2017) 042503 .
[19] X. Mougeot, et al., Phys. Lett. B 718 (2012) 441.
[20] G. Charpak, et al., Nucl. Instrum. Methods 62 (1968) 262.
[21] G. Charpak, et al., Nucl. Instrum. Methods 162 (1979) 405.
[22] E.Yu. Nikolskii, et al., Phys. Rev. C 81 (2010) 064606 .